Acta Crystallographica Section B
Structural Science
ISSN 0108-7681

Ab initio structure determination of 5-anilinomethylene-2,2-dimethyl-1,3-dioxane-4,6-dione from laboratory powder data – a combined use of X-ray, molecular and solid-state DFT study

Ľubomír Smrčok,[a]* Vladimír Jorík,[b] Eva Scholtzová[a] and Viktor Milata[b]

[a]Institute of Inorganic Chemistry, Slovak Academy of Sciences, Dúbravská cesta 9, SK-845 36 Bratislava, Slovakia, and [b]Faculty of Chemical and Food Technology, Slovak University of Technology, Radlinského 9, SK-812 37 Bratislava, Slovakia

Correspondence e-mail: uachsmrk@savba.sk

Received 23 November 2006
Accepted 7 February 2007

The crystal structure of the title compound was solved from laboratory powder diffraction data in the triclinic group $P\bar{1}$ by simulated annealing using the program *DASH*. Since Rietveld refinements yielded inaccurate geometries the structure was finally refined by geometry optimization using energy minimization in the solid state with the DFT/plane-waves approach. The molecule is essentially planar and its Meldrum's acid moiety (2,2-dimethyl-1,3-dioxane-4,6-dione) has a flattened boat conformation. The bond orders in the molecule estimated using a natural bond-orbitals formalism correlate with the optimized bond lengths. The structure in the solid state is based on dimer units in which the molecules are held by N—H···O and C—H···O hydrogen bonds in addition to electrostatic interactions. These units interact through weak C—H···O hydrogen bonds. It is suggested that structure refinement by energy minimization at the DFT level of theory may in many cases successfully replace Rietveld refinement.

1. Introduction

Meldrum's acid (MA), isopropylidenmalonate, 2,2-dimethyl-1,3-dioxane-4,6-dione, is a cyclic isopropylidene ester of malonic acid. It is an active methylene compound with extensive synthetic potential (McNab, 1978; Chen, 1991). Although it was prepared as early as 1908 (Meldrum, 1908), its crystal structure was not reported until much later (Pfluger & Boyle, 1985). The solid-state conformation of the molecule in the orthorhombic structure (*Pbca*) has been shown to be the boat conformation; the molecules in the structure are fixed by weak C—H···O interactions. One possible application of MA is the preparation of 4-quinolones (Gordon *et al.*, 1983) or their fused analogues (Cassis *et al.*, 1985; Saloň *et al.*, 2000, 2001, 2004) starting from its precursors, *N*-substituted 5-aminomethylene MA derivatives. These types of compounds are exploited in the Gould–Jacobs reaction to prepare the well known group of drugs 4-quinolones, which are active antibacterial, anticancerogenic, immunomodulator, antihelmintic and antiparasitic agents in human or veterinary treatments (Milata *et al.*, 2000), or can cause apoptosis (Repický *et al.*, 2005). The simplest compound among the aminomethylene derivatives is the title compound, 5-anilinomethylene (I). Meldrum's acid derivatives belong to a large group of anilinoethylene derivatives with two electron-accepting (withdrawing) substituents on the opposite side to the amino group, *e.g.* in β positions (Hermecz *et al.*, 1992; Kettmann *et al.*, 2004).

© 2007 International Union of Crystallography
Printed in Singapore – all rights reserved

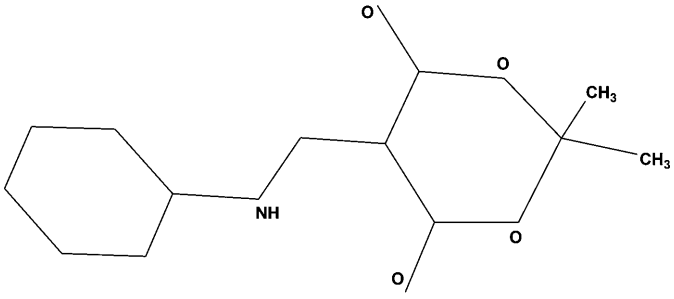

(I)

Several crystal structures of derivatives of MA have been reported, *e.g.* Krapivin *et al.* (1989), Jiang *et al.* (1993), Blake, McNab & Morrow (1994), Blake, Gould *et al.* (1994), Blake *et al.* (1997, 2003), de Armas *et al.* (2000) and Joussef *et al.* (2005). The structures and gas-phase ionization energies of MA and its related cyclic and acyclic compounds have recently been investigated theoretically at the B3LYP and MP2 levels of theory by Lee *et al.* (2003). Their molecular structure optimizations proved the boat configuration to be the most stable for MA *in vacuo*, but upon substitution of the methylene groups the twisted chair or chair gradually became more stable.

The aim of this study was twofold. First, to solve the structure of the title compound from laboratory powder data as it was impossible to prepare single crystals of a suitable size. Secondly, to refine the structure by:

(i) restrained Rietveld refinement and

(ii) structure optimization by energy minimization in the solid state,

and to compare the performances of both approaches. Although the second approach is not yet a widely accepted procedure in the field of powder diffraction, it can be, strictly speaking, called refinement as it improves the accuracy of the quantities of interest starting from their 'rough' estimates. The size of a problem tractable by a solid-state DFT method running on a laboratory computer nowadays reaches 200–300 atoms per unit cell, H atoms included. When the most common space group found for organic structures ($P2_1/c$) is considered, the size of a molecule is then as much as 50–75 atoms, *i.e.* well above the current limit for unrestrained organic powder refinement. The main advantage of such an approach is that the positions of the H atoms are, in contrast to X-ray refinements, optimized along with the positions of the 'heavy' atoms, thus providing reliable hydrogen-bond geometry. In addition, the shape of the molecule obtained by a molecular calculation is further optimized under the constraints imposed by a crystal field. Since theoretical calculations are, as a rule, carried out in the space group $P1$, the simultaneous optimization of the geometries of several molecules within a cell provides a good measure of the internal consistency of the optimization and structure solution.

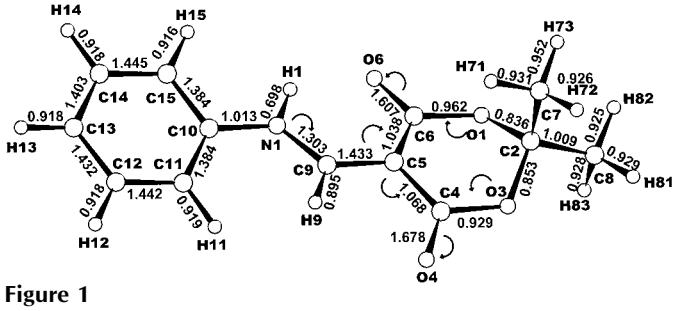

Figure 1
Atom-labeling scheme in a molecule of the title compound. Structure solution involved variation of the following torsional angles: $\tau_1 = C_{11}-C_{10}-N_1-C_9$ and $\tau_2 = C_{10}-N_1-C_9-C_5$. The numbers above the bonds are Wiberg bond orders calculated for the isolated molecule using the NBO formalism. Arrows indicate the predicted electron-density transfer.

2. Synthesis

Aniline (10 mmol, 0.93 g) was added to a solution of 5-methoxy- or ethoxymethylene-2,2-dimethyl-4,6-dioxo-1,3-dioxane (10 mmol; Bihlmayer *et al.*, 1967; Saloň *et al.*, 2000) in ethanol (20 ml) under reflux while starting compounds disappeared (TLC control, eluent chloroform: methanol 10:1). The reaction mixture was then cooled, evaporated on a rotary evaporator and recrystallized from ethanol. Yield 82%, m.p. 429–430 K.

3. Experimental and calculation

The powder pattern used for structure determination and Rietveld refinement was collected within the 2θ range 3–80° with a transmission Stoe Stadi-P diffractometer, using strictly monochromatic Co $K\alpha_1$ radiation. To determine a possible preferred orientation, another pattern was collected by applying the same data collection strategy with a Philips 1730/50 reflection diffractometer using β-filtered Cu $K\alpha$ radiation. The structure was solved by the simulated annealing global optimization procedure, as implemented in the *DASH* program (David *et al.*, 2001) using only the transmission data. Restrained Rietveld refinements were carried out with the *GSAS* package (Larson & Von Dreele, 2000) with an *EXPGUI* interface (Toby, 2001). Molecular geometries were analysed using *PLATON* (Spek, 2003), *MERCURY* (Bruno *et al.*, 2002) and *DIAMOND* (Brandenburg, 2000).

Molecular calculations were performed using the *GAUSSIAN*98 program package (Frisch *et al.*, 1998) at the B3LYP/6-31G** level of theory. NBO (natural bond-orbital) calculations were carried out using the *NBO* 3.1 version (Glendening *et al.*, 1993) of the program included in the *GAUSSIAN*98 package. Solid-state calculations were performed using the Vienna *ab initio* simulation package *VASP* (Kresse & Hafner, 1993 1994*a*; Kresse & Furthmüller, 1996). The exchange–correlation function was expressed in the localized density approximation (LDA) according to Perdew & Zunger (1981), together with the generalized gradient approximation (GGA) according to Perdew & Wang (1992). Plane waves formed a basis set and calculations were performed using the projector-augmented wave method (Blöchl, 1994; Kresse & Joubert, 1999) and using atomic pseudo-potentials (Kresse & Hafner, 1993, 1994*b*). An optional energy cut-off controlling the

Table 1
Experimental details.

Crystal data	
Chemical formula	$C_{13}H_{13}NO_4$
M_r	247.24
Cell setting, space group	Triclinic, $P\bar{1}$
Temperature (K)	300
a, b, c (Å)	10.60310, 11.59680, 5.50320
α, β, γ (°)	97.8790, 103.8910, 71.4570
V (Å^3)	621.43
Z	2
Radiation type	Co $K\alpha_1$
Data collection	
Diffractometer	Stoe Stadi-P
Data collection method	$\theta/2\theta$

accuracy of the calculation was set to 400 eV, representing an extended basis set and consequently highly accurate calculations. The Brillouin-zone sampling was restricted to four k points. The positions of all the atoms were optimized by applying the conjugate-gradient method until the differences in total energy were less than 10^{-5} eV. No symmetry restrictions were applied during the geometry optimization; the structure optimization was thus effectively performed in the $P1$ space group.

4. Indexing, structure determination and refinement

The experimental details are given in Table 1. The transmission pattern was independently indexed in two Laboratories using the program *ITO* (Visser, 1969). Both calculations gave triclinic cells with very similar cell parameters and the average $M_{20} \simeq 46$. The space group $P\bar{1}$ was assigned, taking into account the cell volume and density. The $P1$ space group was not considered because it was expected that a possible deviation from the $P\bar{1}$ symmetry would be later disclosed by structure refinement with energy minimization. The accuracy of the estimated lattice parameters was further improved by several cycles of the LeBail pattern decomposition method. Considering a heavy overlap of diffractions at high angles, the original 2θ range was for the structure solution with an upper limit of 50° 2θ. The pattern was corrected for background and after several cycles of Pawley fitting (Pawley, 1981) $\chi^2_{\rm Pawley}$ dropped to a value which is very acceptable for laboratory data, ~ 9. The structure was then solved by simulated annealing varying, in addition to three positional parameters and four quarternions, two torsional angles (Fig. 1). The H atoms were also included in the structure search as they contribute $13e^-$ per molecule to the total electron density. To avoid geometrical inaccuracies in the molecular model, its geometry was fully optimized prior to structure solution (convergence in total energy $\Delta E < 10^{-4}$ a.u.). Several structure solutions gave very close time variations of the minimized quantity ($\chi^2_{\rm SA}$) and very similar final values, all near 28. Since the resulting molecular packing was reasonable, a series of Rietveld refinements was carried out. Background variation was described by a Chebyshev polynomial and the pseudo-Voigt profile function was used to approximate the profiles. Inasmuch as a comparison of the reflection and transmission patterns suggested [121] to be a possible direction of the preferred orientation, the March–Dollase correction (Dollase, 1986) was also attempted in the first stage. All the positions of the non-H atoms were refined with the support of a set of bond length and angle restraints. The restraints were based on a geometrical analysis of the molecular geometry obtained by energy minimization *in vacuo*. The planarity of the benzene ring and part of MA (C4—C6—O1—O3) was supported by two additional planarity restraints. The total impact of the restraints on the refinements was controlled by a common weighting factor WX.[1] Three X values were used: 50 for heavily restrained refinements, 5 for moderately restrained and 0 for unrestrained refinements. The H atoms were refined riding on heavy atoms, keeping the C/N—H distances equal to 1 Å. The isotropic displacement parameters U(iso) of the H atoms were assigned the values 1.2 times U(iso) of the parent heavy atoms. Inasmuch as the number of refined parameters was rather large for a powder refinement, one series of refinements was carried out by releasing the positional and displacement parameters alternately until convergence was achieved. The results obtained in this series are referred to as X/U hereafter. The second series was carried out with all atomic parameters released simultaneously ($X + U$). The number of refined atomic parameters was 55 or 73, respectively. Since the refined values of the March–Dollase parameter were not significantly different from 1.0, this parameter was omitted from the last refinement cycles. An example of the Rietveld fit is shown in Fig. 2. Parallel to the Rietveld refinements, the energy calculations at both the molecular and crystal level were carried out for all the relevant configurations. These single-point calculations were carried out with the atomic coordinates fixed at the values obtained in the respective Rietveld refinements.

5. Results and discussion

5.1. Accuracy of the refinements

The basic information for all the calculations is summarized in Table 2. As the scales of the total energies for the molecular and solid-state calculations are different, the individual energies are reported relative (ΔE) to the respective reference values – the lowest energy within a series. In general, the differences in the molecular energies mainly reflect the changes in bond distances and angles, and to a much lesser extent the changes in torsional angles. In the solid state any variations in cell energies also reflect these changes in the molecular geometry, which are due to crystal packing and/or the formation of hydrogen bonds.

The lowest molecular energy corresponds to the molecular geometry *in vacuo*. Inasmuch as during structure solution the molecular geometry could be modified only by varying two torsional angles (Fig. 1), the increase in molecular energy of 0.16 eV is attributed to the small changes in the mutual

[1] For details see the *GSAS* Technical Manual.

Table 2
Rietveld factors of agreement, differential energies (eV), $\Delta E = E - E_{ref}$, and Meldrum's acid ring conformations.

Reference energy values are E_{ref} (molecule, M) = −23371.95 eV, E_{ref} (solid, S) = −401.28 eV. 1 eV = 96.55 kJ mol^{-1}, FB – flattened boat

Refinement or computational model	R_{wp}	R_{F^2}	S	ΔE(M)	ΔE(S)	MA conformation
Molecule				*Reference*		FB
Solved structure				0.16	0.49	
Solved and optimized					*Reference*	FB
*W*0(*X*/*U*)	0.04	0.07	2.2	8.45	15.96	Undefined
*W*5(*X*/*U*)	0.04	0.08	2.3	2.05	4.39	Deformed FB
*W*50(*X*/*U*)	0.04	0.09	2.4	0.75	1.82	Deformed FB
*W*0(*X* + *U*)	0.04	0.08	2.2	10.03	18.93	Undefined
*W*5(*X* + *U*)	0.04	0.09	2.3	1.52	3.31	Deformed FB
*W*50(*X* + *U*)	0.05	0.10	2.5	0.98	2.26	Deformed FB

orientation of the phenyl ring and the MA residue. The cell energy of the solved structure is very close (∼ 0.5 eV) to the reference value, which was obtained by the subsequent optimization of all the atomic positions in the cell by energy minimization. The overall trends in the molecular and cell energies, obtained from single-point calculations based on the atomic coordinates taken from Rietveld refinements, are such that the energies increase with:

(i) the decreasing impact of restraints and

(ii) the increasing number of simultaneously refined atomic parameters.

These trends in total energies are in contrast to the nearly identical values of the Rietveld factors of agreement not reflecting changes in the structures. To complete the first picture it should be noted that for *W*0(*X* + *U*) the Rietveld refinement gave O1(O3)—C2 bond distances longer than 1.94 Å, *i.e.* in fact it tore the molecule into two parts.

Increasing energies are mirrored by the increasing relative errors of the individual bond distances summarized in median-based box-and-whisker plots (Fig. 3). Two unrestrained refinements resulted in unacceptable relative errors, *W*0(*X* + *U*) with larger errors due to the larger number of simultaneously refined parameters. The refinements applying restraints weighted by the factor five (*W*5) provided bond distances, whose relative errors are acceptable for the majority of powder refinements, where accuracy comparable to single-crystal refinement is neither requested nor expected. From Fig. 3 it is also evident that only heavily restrained refinements (*W*50) gave distances which are in fair agreement with the reference values. The size of the 50% box corresponding to the refinement carried out by energy minimization is comparable to those derived from two tightly restrained Rietveld refinements. Closer inspection of the values summarized in the boxes showed that while for Rietveld refinements the distribution of relative errors is not systematic, for energy minimization the largest relative errors are systematically in the C—O distances. This artefact we attribute to the slightly different quality of the atomic pseudopotentials used in the calculations by *VASP*.

Table 3 summarizes the deviations from the expected planarity of the phenyl ring and the deviations from 120° of the ring bond angles. While for the *W*50 and *W*5 refinements all the deviations are tolerable, unrestrained *W*0 refinements gave deviations beyond acceptable limits. In contrast, a geometrically unrestrained energy-minimization calculation provided almost ideal ring geometry. Larger deviations in bond angles around the N1 atom from the expected are due to the different nature of the substituents attached to it and hence reflect different bonding conditions. Finally, a summary of isotropic displacement parameters *U* showed that *X*/*U* refinements provided consistent (though most probably inaccurate) estimates, which are independent of the

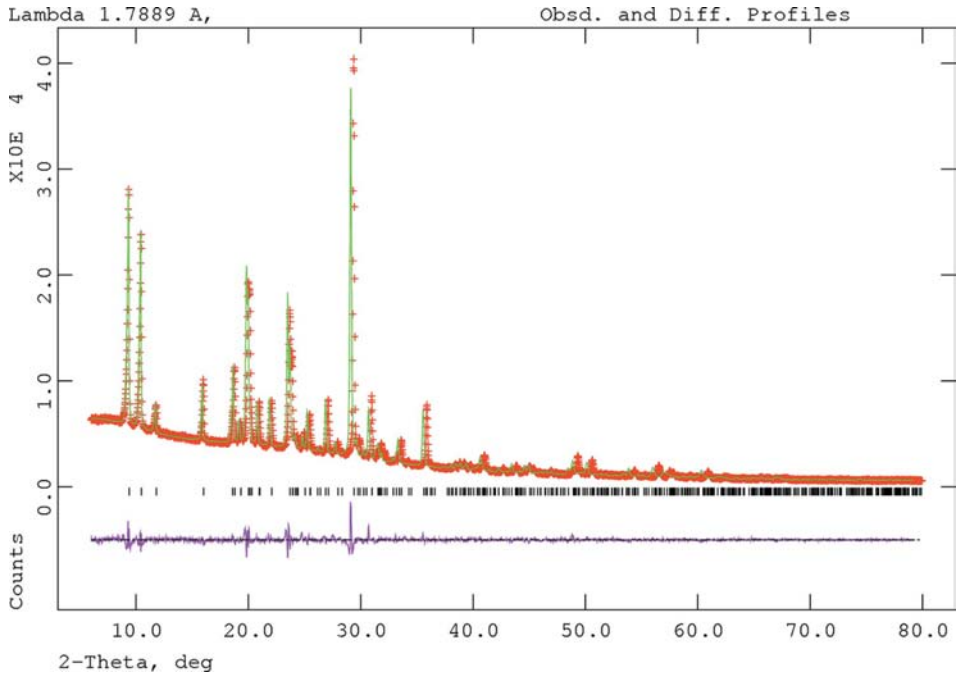

Figure 2
Final observed (crosses), calculated (solid line) and difference (below) diffraction profile for W50(*X* + *U*) Rietveld refinement of (I).

Table 3
Deviations of atoms ($\Delta P \times 1000$ Å) from the plane defined by C10–C15 + N1 atoms and deviations of phenyl ring bond angles ($\Delta\varphi$ °) from 120°.

The latter also include the C15—C10—N1 and C11—C10—N1 bond-angle deviations for Rietveld refinements, while for DFT solid state and molecular geometry optimizations two sets are reported, because the values of optimized C—C—N bond angles significantly differ from the values of the C—C—C bond angles E_{min}(M), E_{min}(S). The geometric parameters in molecule (M) and structure (S) were obtained by energy minimization. Deviations are reported as (minimum, median, maximum) values for every calculation.

Calculation	ΔP	$\Delta\varphi$
*W*50(*X*/*U*)	−2, 1, 3	−0.2, 0, 0.3
*W*5	−24, −3, 21	−1.5, 0.1, 1.3
*W*0	−290, 0, 560	−20, −1.5, 18
*W*50(*X* + *U*)	−29, −4, 15	−0.4, 0, 0.3
*W*5	−36, −1, 23	−1.4, 0.8, 0.9
*W*0	−230, −40, 240	−31, −3, 12
E_{min}(S)	−5, −1, 23	−0.5, 0.1, 0.5†
		−2.6, 0.1, 2.6‡
E_{min}(M)	−5, 2, 3	−0.6, 0.1, 0.8†
		−2.4, 0.1, 2.7‡

† C—C—C angles only. ‡ C—C—C + C—C—N angles.

Table 4
Selected bond lengths (Å), bond angles (°) and torsion angles (°).

Calculated bond distances were rounded to the third decimal place and bond angles to the first, in keeping with the typical precision of experimentally determined values. As the values of the individual C—C bond lengths in the phenyl ring are very similar, only the mean value and the corresponding standard uncertainties are given.

O1—C6	1.377	C6—O1—C2	117.5
O1—C2	1.466	C4—O3—C2	118.2
O3—C4	1.384	C10—N1—C9	125.8
O3—C2	1.462	N1—C10—C15	122.6
O4—C4	1.249	N1—C10—C11	117.5
O6—C6	1.255	N1—C9—C5	125.5
N1—C10	1.411	O3—C4—C5	116.4
N1—C9	1.326	O3—C4—O4	117.6
C5—C9	1.392	O4—C4—C5	125.9
C4—C5	1.448	O1—C6—C5	117.6
C5—C6	1.438	O1—C6—O6	117.6
C2—C7	1.513	O6—C6—C5	124.8
C2—C8	1.507	O1—C2—C7	109.9
N1—H1	1.040	O1—C2—C8	105.9
C—H (all)	1.090	O3—C2—C8	106.5
		O3—C2—C7	110.2
⟨C—C⟩ phenyl	1.395 (3)	O1—C2—O3	109.9
C11—C10—N1—C9	166.4		
C10—N1—C9—C5	179.8		

common weighting factor *WX*. On the contrary, $X + U$ models suffer from the same problem as the majority of powder refinements – the *U* values vary wildly from atom to atom and negative values appear in an unpredictable manner.

Considering the results from all the refinements it was concluded that the most accurate structure was obtained by unrestricted geometry optimization by energy minimization in the solid state. Geometrical analysis using *PLATON* (Spek, 2003) revealed that the symmetry of the structure can be increased from $P1$ to $P\bar{1}$, as the root mean-square deviations between atomic coordinates of the two molecules were zero. Atom coordinates have been deposited,[2] Table 4 depicts selected bond distances, angles and torsion angles. Hydrogen bonds are summarized in Table 5.

5.2. Electronic, molecular and crystal structure

NBO (natural bond orbital) analysis (Foster & Weinhold, 1980) of the molecular electronic structure revealed (Fig. 1) that the bond order of N1—C9 is intermediate between a single and a double bond (1.303). The higher bond order results from an involvement of the lone pair of N1 in the delocalization of electrons in the middle part of (I). A detailed analysis of NBO results showed that the electron donor, the N1 atom lone pair, is connected through a formally double C5═C9 bond to electron-withdrawing ('pull') carbonyl groups. As a result, the electrons from the lone pair are delocalized to a formally single N1—C9 bond, giving it a partially double-bond character. Furthermore, π-electrons from the double C5═C9 bond are pulled towards the C5—C6 and C4—C5 bonds, which gain a slightly multiple character. Free electron pairs of O1 and O3 atoms are delocalized to the O1—C6 and O3—C4 bonds, respectively, and also interact with anti-bonding NBOs of the nearest σ-bonds. These interactions are responsible for back-transferring the electron density to σ-bonds, thus counterbalancing the withdrawal of π-electrons and lone pairs by carbonyl groups. The geometrical consequence of such electron redistribution is the elongation of the C4—O4, C6—O6 and C9—C5 bonds and the

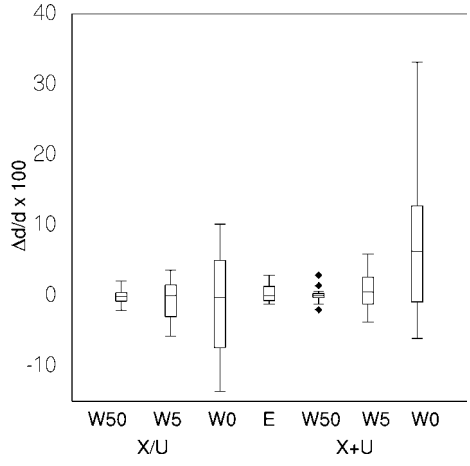

Figure 3
Distribution of the relative errors, $\Delta d/d$ (where $\Delta d = d - d_{ref}$), of the bond distances between non-H atoms for all the refinements displayed as a box-and-whisker plot. In this type of plot boxes cover the data between the lower and upper quartiles with a median value lying between them. Whisker indicates the lower and upper extremes of the distribution, outliers are marked separately. For the reference values the distances obtained by the optimization of molecular geometry were used. From left to right: three boxes for *X*/*U* Rietveld refinements are separated from the results of $X + U$ refinements by the box corresponding to energy minimization in the solid state (*E*). Diamonds in the *W*50($X + U$) case indicate outliers.

[2] Supplementary data for this paper are available from the IUCr electronic archives (Reference: AV5081). Services for accessing these data are described at the back of the journal.

Table 5
Hydrogen-bonding parameters (Å, °).

D—H···A	D—H	H···A	D···A	D—H···A
N1—H1···O6	1.04	1.95	2.727	129
N1—H1···O6^{i}	1.04	2.45	3.388	150
C11—H11···O1^{i}	1.09	2.43	3.382	145
C11—H11···O6^{i}	1.09	2.30	3.314	154
C14—H14···O4^{ii}	1.09	2.23	3.246	154
C7—H72···O4^{iii}	1.10	2.36	3.452	173

Symmetry codes: (i) $-x, -y, 1-z$; (ii) $1-x, -y, -z$; (iii) $-x, 1-y, -z$.

shortening of the N1—C9, C4—C5 and C5—C6 bonds. For comparison, NBO analysis for a similar compound having sulfur in place of nitrogen, 2,2-dimethyl-5-(phenylthiomethylene)-1,3-dioxane-4,6-dione (Blake, McNab & Morrow, 1994), was calculated at the same level of theory. The analysis revealed an electron-density distribution similar to that in (I), the main difference being the higher bond order (1.625) of the C7—C5 bond compared with 1.433 found for its structural counterpart in (I), C5—C9. The larger value is explained by the greater involvement of one of the two lone pairs of the S atom to electron delocalization.

The molecule of (I) is essentially planar, torsion angles τ_1 and τ_2 being ~ 166 and $\sim 180^\circ$, respectively. The rotational barrier about the C5—C9 bond was found to be ~ 188.41 kJ mol^{-1} by a stepwise rotation of the MA moiety, *i.e.* by variation of the C6—C5—C9—N1 torsion angle followed by molecular single-point energy calculations *in vacuo*. The influence of the intermolecular hydrogen bond on the planarity of (I) was estimated using a simple computational model, where the environment of (I) was modelled by the MA moiety of the neighbouring molecule of (I) forming an N1—H1···O6^{i} hydrogen bond (Fig. 4). This hydrogen bond further stabilizes the planarity of (I) by an additional ~ 18.84 kJ mol^{-1}. The largest deviation from the best plane fit to all the C atoms of the phenyl ring is negligible, 0.007 Å (C10). The C2 and C5 atoms positioned above the best plane defined for the MA moiety (by O1, O3, C4 and C6 atoms) for 0.084 and 0.550 Å clearly portray its one-side flattened boat conformation.

Geometrical analysis of the MA moieties appearing in the structures of MA derivatives listed in §1 revealed conformations close to that in (I). The only exception was the structure of diethyl-2,2-dimethyl-4,6-dioxo-1,3-dioxane-5,5-diacetate (Jiang *et al.*, 1993), where the MA moiety was reported to be planar. We confirmed this conformation by a molecular geometry optimization at the B3LYP level of theory. In the context of other structures there is not, however, any rational explanation for MA being completely planar. To analyze the conformational behaviour of the MA moiety in (I) another series of molecular calculations was carried out with the aim of looking for configurations which could be energetically closer to that found by structure solution, but with the MA moiety having a different shape. Starting molecular models were prepared by changing the initial value of the C2—O1—C6—C5 torsional angle from a half-chair to a boat conformation. After geometry optimizations this angle was found in all cases to be close to -19° [*cf.* to -21° in the structure of (I)] and the differences in the individual total energies were negligible.

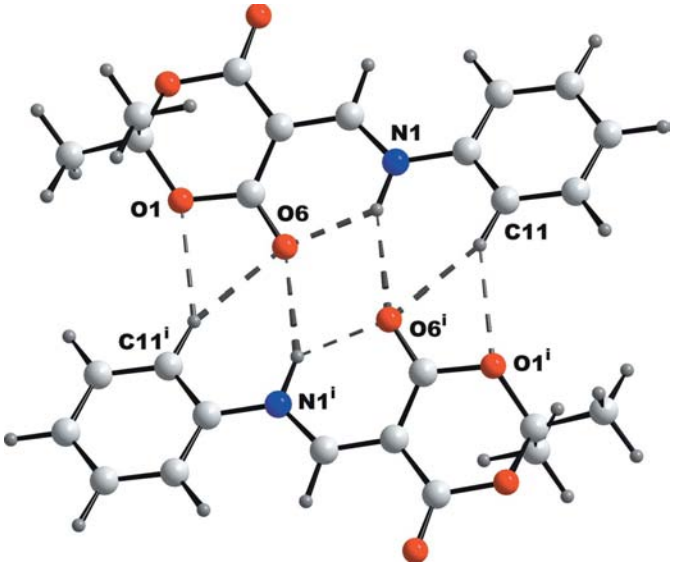

Figure 4
Part of the structure showing the formation of a dimer. Dashed lines represent hydrogen bonds. Symmetry codes: (i) $-x, -y, 1-z$; (ii) $1-x, -y, -z$; (iii) $-x, 1-y, -z$.

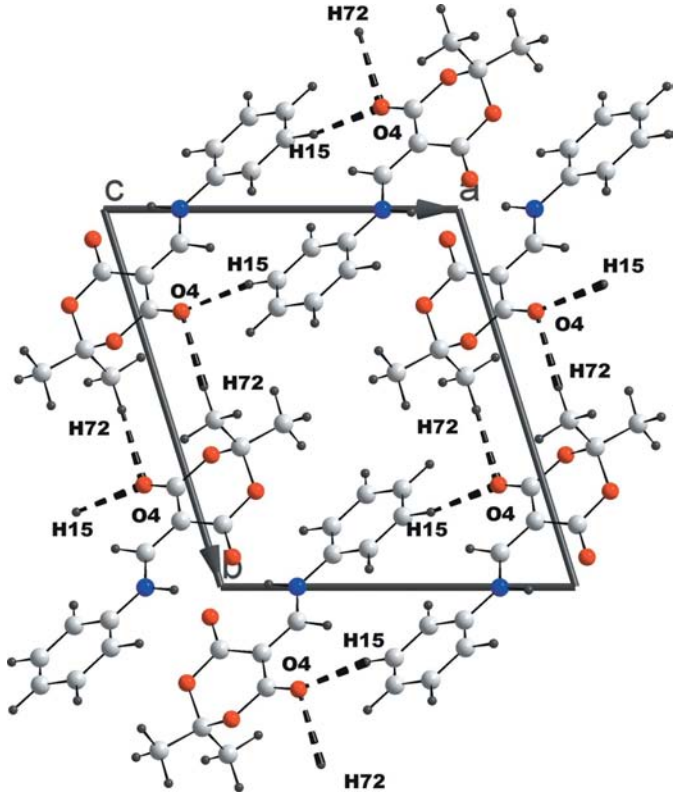

Figure 5
View of the crystal structure of (I) along **c** showing the formation of C—H···O contacts between dimers. The hydrogen bonds within the dimers are omitted for the sake of clarity.

Molecules of (I) are arranged in an antiparallel fashion to dimers. In addition to long-range electrostatic forces [the dipole moment of (I) is 2.9 D], molecules in dimers are held by bifurcated N—H···O and C—H···O hydrogen bonds (Fig. 4). The hydrogen-bond array is completed by C14—H14···O4^{ii} and C7—H72···O4^{iii} weak contacts linking dimer units. The geometric parameters of all the C—H···O bonds fall into the ranges expected for this type of bond: d(H···O) = 2.1–2.5 and d(C···O) = 3.1–3.5 Å (Castellano, 2004). The values of the almost linear C—H···O bond angles point to the prevalence of the electrostatic rather than the van der Waals contribution to the total bond energy (Steiner & Desiraju, 1998; Gatti *et al.*, 2002). A perspective view of these interactions is depicted in Fig. 5. A comparison of d(H···A) distances in the N—H···O hydrogen bonds (Table 5) shows that intramolecular d(H1···O6) is significantly shorter than intermolecular d(H1···O6^{i}). This difference is in accordance with the results of the survey of N—H···O=C bonds (Taylor *et al.*, 1984). Similar dimers are formed for instance in two *N*-aminoazolylmethylene derivatives of MA (Blake, Gould, Irving, McNab & Morrow, 1994). While the reported intramolecular d(N···O) distances of 2.746 (5) and 2.710 (3) Å agree well with the N1···O6 contact distance in (I), the intermolecular N···O distances of 2.917 (5) and 2.902 (3) Å are significantly shorter than the N1···O6^{i} contact distance.

6. Conclusion

Solid-state DFT methods could provide a good alternative to infrequently used rigid-body powder refinement, whose usage in daily practice is limited by factors such as an unfriendly implementation or the limited radius of convergence compared with a 'standard' refinement. The main disadvantage of the structure refinement by energy minimization, although highly disputable, is that a calculation may take hours or days depending on the method and/or computer speed, compared with seconds or minutes for the Rietveld refinement. However, if several structures are not to be solved and refined per day, the length of calculation is far from being critical.

This work was partially supported by Slovak Grant Agency VEGA under the contracts 2/6178/26, 1/2448/05 and by the Science and Technology Assistance Agency (No. APVV-20-007304). ES and LS are grateful to Professor J. Hafner for providing them with a copy of the program *VASP*. Comments and suggestions delivered by referees helped to improve the style of the paper.

References

Armas, H. N. de, Blaton, N. M., Peeters, O. M., De Ranter, C. J., Suárez, M., Ochoa, E., Verdecia, Y. & Salfarán, E. (2000). *J. Chem. Crystallogr.* **30**, 189–194.
Bihlmayer, G. A., Derflinger, G., Derkosch, J. & Polansky, O. E. (1967). *Monatsh. Chem.* **98**, 564–578.
Blake, A. J., Gould, R. O., Irving, I., McNab, H. & Morrow, M. (1994). *Acta Cryst.* C**50**, 1935–1938.
Blake, A. J., McNab, H. & Morrow, M. (1994). *Acta Cryst.* C**50**, 1716–1717.
Blake, A. J., McNab, H., Parsons, S. & Withell, K. (1997). *Acta Cryst.* C**53**, 1956–1958.
Blake, A. J., McNab, H. & Withell, K. (2003). *Acta Cryst.* E**59**, o841–o842.
Blöchl, P. E. (1994). *Phys. Rev.* B**50**, 17953–17979.
Brandenburg, K. (2000). *DIAMOND*, Version 2.1.d. Crystal Impact GbR, Bonn, Germany.
Bruno, I. J., Cole, J. C., Edgington, P. R., Kessler, M. K., Macrae, C. F., McCabe, P., Pearson, J. & Taylor, R. (2002). *Acta Cryst.* B**58**, 389–397.
Cassis, R., Tapia, R. & Valderrama, J. A. (1985). *Synth. Commun.* **15**, 125–133.
Castellano, R. K. (2004). *Curr. Org. Chem.* **8**, 845–865.
Chen, B. C. (1991). *Heterocycles*, **32**, 529–597.
David, W. I. F., Shankland, K., Cole, J., Maginn, S., Motherwell, W. D. S. & Taylor, R. (2001). *DASH*, Version 3.0. Cambridge Crystallographic Data Centre, 12 Union Road, Cambridge, England.
Dollase, W. A. (1986). *J. Appl. Cryst.* **19**, 267–272.
Foster, J. P. & Weinhold, F. (1980). *J. Am. Chem. Soc.* **102**, 7211–7218.
Frisch, M. J. *et al.* (1988). *GAUSSIAN*98, Revision A.7. Gaussian, Inc., Pittsburgh PA, USA.
Gatti, C., May, E., Destro, R. & Cargnoni, F. (2002). *J. Phys. Chem. A*, **106**, 2707–2720.
Glendening, E. D., Reed, A. D., Carpenter, J. E. & Weinhold, F. (1993). *NBO*, Version 3.1. Theoretical Chemistry Institute, University of Wisconsin, Madison, Wisconsin, USA.
Gordon, H. J., Martin, J. C. & McNab, H. (1983). *J. Chem. Soc. Chem. Commun.* **17**, 957–958.
Hermecz, I., Keresztúri, G. & Vasvári-Debreczy, L. (1992). *Advances in Heterocyclic Chemistry*, edited by A. R. Katritzky, Vol. 54. New York: Academic Press Inc.
Jiang, A., Hong, L., See, R. F. & Churchill, M. R. (1993). *Acta Cryst.* C**49**, 1000–1001.
Joussef, A. C., da Silva, L. E., Bortoluzzi, A. J. & Foro, S. (2005). *Acta Cryst.* E**61**, o2873–o2874.
Kettmann, V., Lokaj, J., Milata, V., Marko, M. & Štvrtecká, M. (2004). *Acta Cryst.* C**60**, o252–o254.
Krapivin, G. D., Zavodnik, V. E., Valter, N. I., Belsky, V. K. & Kulnevich, V. G. (1989). *Khim. Geterotsikl. Soed.* **9**, 1201–1207 (in Russian).
Kresse, G. & Furthmüller, J. (1996). *Comput. Mater. Sci.* **6**, 15–50.
Kresse, G. & Hafner, J. (1993). *Phys. Rev. B*, **47**, 558–561.
Kresse, G. & Hafner, J. (1994*a*). *Phys. Rev. B*, **49**, 14251–14269.
Kresse, G. & Hafner, J. (1994*b*). *J. Phys. Condens. Matter*, **6**, 8245–8527.
Kresse, G. & Joubert, D. (1999). *Phys. Rev. B*, **59**, 1758–1775.
Larson, A. C. & Von Dreele, R. B. (2000). *GSAS*, Report LAUR 86–748. Los Alamos National Laboratory, New Mexico, USA.
Lee, I., Han, I. S., Kim, Ch. K. & Lee, H. W. (2003). *Bull. Korean Chem. Soc.* **24**, 1141–1149.
McNab, H. (1978). *Chem. Soc. Rev.* **7**, 345–358.
Meldrum, A. N. (1908). *J. Chem. Soc.* **93**, 598–601.
Milata, V., Claramunt, R. M., Elguero, J. & Zálupský, P. (2000). *Targets Heterocycl. Syst.* **4**, 167–203.
Pawley, G. S. (1981). *J. Appl. Cryst.* **14**, 357–361.
Perdew, J. P. & Wang, Y. (1992). *Phys. Rev. B*, **45**, 13244–13249.
Perdew, J. P. & Zunger, A. (1981). *Phys. Rev. B*, **23**, 5048–5079.
Pfluger, C. E. & Boyle, P. D. (1985). *J. Chem. Soc. Perkin Trans. II*, pp. 1547–1549.
Repický, A., Jantová, S., Theiszová, M. & Milata, V. (2005). *Biomed. Pap.* **49**, 345–347.
Saloň, J., Milata, V., Chudík, M., Prónayová, N., Leško, J., Seman, M. & Belicová, A. (2004). *Monatsh. Chem.* **135**, 283–291.
Saloň, J., Milata, V., Prónayová, N. & Leško, J. (2000). *Monatsh. Chem.* **131**, 293–299.

Saloň, J., Milata, V., Prónayová, N. & Leško, J. (2001). *Collect. Czechoslov. Chem. Commun.* **66**, 1691–1697.
Spek, A. L. (2003). *J. Appl. Cryst.* **36**, 7–13.
Steiner, T. & Desiraju, G. R. (1998). *Chem. Commun.* pp. 891–892.
Taylor, R., Kennard, O. & Versichel, W. (1984). *Acta Cryst.* B**40**, 280–288.
Toby, B. H. (2001). *J. Appl. Cryst.* **34**, 210–213.
Visser, J. W. (1969). *J. Appl. Cryst.* **2**, 89–95.